

Thesis

Design of a planar coil and reader for temperature measurement

R.W.C. Hamelink



THESIS

DESIGN OF A PLANAR COIL AND READER FOR TEMPERATURE MEASUREMENT

by

R.W.C. Hamelink

in partial fulfillment of the requirements for the degree of

Bachelor of engineering
in Electrical engineering

at the Delft University of Technology Biomedical electronics group,
to be defended publicly on Friday June 27, 2014 at 10:00 AM.

Supervisor:	prof. dr. ir. W. Serdijn,	TU Delft
2nd Supervisor:	ir. A. L. Mansano,	TU Delft
Thesis committee:	ing. J. E. J. op den Brouw,	HHS Delft
	ing. Duijvenvoorde,	HHS Delft

SUMMARY

At the biomedical department of the TUDelft a sensor node is designed[1]. This is an Autonomous Wireless Sensor Node(AWSN) with temperature monitoring, which is powered up wirelessly and have data transmission through backscattering. The aim of the project is to design a receiver for the AWSN and to design a applicable coil for the energy harvesting.

The coil is calculated, with use of different formulas found in literature. Also the coil is simulated to have a more accurate idea of the parameters. From the calculations and simulations results two designs, rectangular and hexagonal, are proposed.

From measurements the signal strength is known. Given the signal strength the receiver blocks are determined. There are two main blocks of which the receiver consists, a RF-frontend and a LF-backend. These blocks are turned into circuitry and simulated. In simulation everything is working, however there is still a problem with the buffer. After simulation the different parts were tested. A complete test is missing due to noise environment which could not be solved yet. However the RF-frontend completely is working and reaches the requirements. In the LF-backend the buffer is distorting the signal, and a lot of 100MHz noise is induced into the circuit.

ACKNOWLEDGEMENTS

Without the help of some people this work could not be done. First of all I want to thank prof. Wouter Serdijn to give me the opportunity to do a project for his research group, the biomedical electronics group at TUDelft. You gave me the possibility to do a project in what I like and wanted to learn more, namely RF and analog design.

Also I want to really thank Andre Mansano, my daily supervisor. Thanks for the lots of time you spend to explain electronics to me, and helping me when were in the lab debugging;). Every time I want to ask you something you took your time for me. Hopefully this work can contribute to your promotion. I look forward to it!

CONTENTS

Summary	iii
Acknowledgements	v
List of Figures	ix
List of Tables	xi
1 Introduction	1
1.1 Problem description	1
1.1.1 Requirements	1
1.2 Structure of the thesis	2
2 System Design	3
2.1 Coil for energy harvesting	3
2.1.1 Working principle	3
2.1.2 Coil calculations	4
2.2 Data link	6
2.2.1 Received signal.	7
2.3 Receiver.	8
2.3.1 LNA	8
2.3.2 Band-pass filter	8
2.3.3 Envelope detection	9
2.3.4 Buffer, band-pass filter and amplifier	9
2.3.5 Averaging and comparator	9
3 Circuit design	11
3.1 Implementation	11
3.1.1 LNA	11
3.1.2 RF filtering.	12
3.1.3 Envelope detection	13
3.1.4 Buffer, filter and amplifier	13
3.1.5 Averaging	14
3.1.6 Comparator	14
3.2 Conclusion	15
3.2.1 Complete circuit	15
4 Circuit simulation	17
4.1 Coil simulation	17
4.2 Receiver simulations	17
4.2.1 Simulink	18
4.2.2 RF-frontend simulations.	19
4.2.3 LF-backend simulations	21
4.2.4 Buffer	21
4.2.5 Filter	22
4.2.6 Amplifier.	23
4.2.7 Averaging	23
4.2.8 Comparator	24
4.2.9 Complete LF-backend	24

5	Measurements	25
5.1	Link losses	25
5.2	LNA's	26
5.3	SAW filter	28
5.4	RF front-end noise figure and gain	29
5.5	Measurement setup envelope detector	31
5.5.1	Envelope detector	31
5.6	LF-backend	32
6	Conclusions and future work	35
6.1	Conclusions.	35
6.2	Recommendations	35
A	Coil Simulation and Calculation results	37
	Bibliography	41

LIST OF FIGURES

2.1	Calculated AC resistance for different number of turns and increased trace width and spacing	6
2.2	Backscattered signal from AWSN node	7
2.3	Calculated link losses for different distances	8
2.4	Block diagram of receiver circuit	8
3.2	Preview of program PASAN	12
3.3	Matching network for second LNA	12
3.4	LF circuit with buffer, LPF and amplifier	13
3.5	Averaging circuit	14
3.6	Comparator circuit	14
3.7	Complete proposed LF circuit	15
4.1	Matlab Simulink model of proposed receiver design	18
4.2	Simulink simulation results	18
4.3	Simulink simulation results	19
4.4	S(1,1), S(1,2), S(2,1) and S(2,2) of the LNA1 with matching network	19
4.5	S(1,1), S(1,2), S(2,1) and S(2,2) of the LNA2 with matching network	20
4.6	S(1,1), S(1,2), S(2,1) and S(2,2) of the LNA2 with matching network	20
4.7	S(1,1), S(1,2), S(2,1) and S(2,2) of the SAW filter	21
4.8	Inputsignal of the LF-backend	21
4.9	Output signal of buffer	22
4.10	Filter characteristics of the LF filter	22
4.11	Inputsignal of the LF-backend	22
4.12	Inputsignal of the LF-backend	23
4.14	Comparator output of the LF-backend	24
4.15	Inputsignal of the LF-backend	24
5.1	Measurement setup for measuring the signal losses in air	25
5.2	Measurement result of received signal signal	26
5.3	S-parameters LNA1	27
5.4	S-parameters LNA2 without matching network	27
5.5	S-parameters LNA3 with matching network	28
5.6	S-parameters SAW filter	29
5.7	S-parameters of measurement of LNA1, SAW filter, and LNA2	29
5.8	NF and gain plots from receiver	30
5.10	Envelope(50kHz) detected by envelope detector only	32
5.11	Envelope(500kHz) detected by envelope detector with whole RF-frontend	32
5.12	Input signal for LF backend with noise and determined frequency of the noise	33
5.13	Signal that is coming out of the buffer in the LF-backend	33
5.14	Filtered signal before amplifier in the LF-backend	33
5.15	Filtered signal before amplifier in the LF-backend	34
5.16	Filtered signal before amplifier in the LF-backend	34
A.1	Calculated inductance for circular coils with different approaches	38
A.2	Calculated inductance for rectangular coils with different approaches	38

LIST OF TABLES

2.1	Used dimensions of different coils	5
2.2	Calculated number of turns for an inductance as close as possible to $9.348\mu H$	5
2.3	Parameters used for calculating link losses of backscattered signal	7
3.1	Specification of the SAW filter	12
3.2	Specification of the envelope detector	13
4.1	Derived simulation results for hexagonal and rectangular coil	17
5.1	Characteristics of used antenna for measuring link losses	25
5.2	Measurement setup link losses	26
5.3	Measurement setup LNA	26
5.4	Comparison between simulation and measured S-parameters LNA1	26
5.5	Comparison between simulation and measured S-parameters LNA2 and LNA3	27
5.6	Measurement setup SAW filter	28
5.7	Comparison between simulation and measured S-parameters SAW filter	28
5.8	Measurement setup RF front-end	30
5.9	Measurement setup envelope detector	31
5.10	Measurement setup LF-backend	32
A.1	Simulation results of energy harvesting coil in circled and hexagonal shape	39
A.2	Simulation results of energyharvesting coil in rectangle shape	39

1

INTRODUCTION

In 1999 and 2009, the internet was filled with ideas and information of humans. However humanity(or just things) itself were not part of it, and that was what Kevin Ashton wanted to make clear with the term "Internet of Things' (IoT).[2]. He asked himself why we were not connecting "things" to the internet instead of ideas and information? Information is important, and it should be gathered by computers not by humans. This is the idea of IoT: All things and people are connected to each other with the least possible human intervention.

The IoT philosophy generates a wide range of possibilities to improve our environment. For example a patient that can be monitored continuously. With this data, data can be collected, recorded and analyzed. This can improve preventive care of a patient, diagnosis of the patient and improve research to patients(pharmacological), increasing the quality of care.

To create such a medical environment where all kinds of patients physiological parameters are measured and processed, sensor nodes are key elements in the IoT. And without these sensor nodes the IoT cannot interpret it's environment.

1.1. PROBLEM DESCRIPTION

At the biomedical department of the TUDelft a sensor node is designed[1]. This is an Autonomous Wireless Sensor Node(AWSN) with temperature monitoring, which is powered up wirelessly and have data transmission through backscattering. The sensor node is dual band, one band for energy harvesting(ISM band) and one for data transmission(MICS band). This dual band structure allows the node for simultaneously energy harvesting and data transmission. The AWSN has been tested in the laboratory with an oscilloscope to read the temperature information. For power link a coil with the size of a credit card has been used. However, in real medical application a receiver is needed to read information, replacing the oscilloscope and a small coil need to be implemented (two euros coin size).

1.1.1. REQUIREMENTS

From the need of a practical application for the AWSN a energy harvesting coil and receiver are designed. The requirements, also derived from [1] for both the receiver and coil are:

Specifications of the AWSN

- Modulation type: OOK
- Baseband of 50kHz
- Minimum transmitted power for energy harvesting: $-18.2 \pm 1.0\text{dBm}$
- Maximum transmitted power for data transmission: -16dBm

Requirements of the coil are:

- As close as possible to the exact impedance of the IC, namely $9.5\mu H$ and 12Ω

- Should fit the size of a normal bandage or a 2 euro coin
- Maximum thickness of the coil must not exceed 2/3 coins stacked together

Requirements of the receiver are:

- Capable of receiving the signal at a distance of 10–20 cm.
- Only receive the signal of the AWSN
- Demodulate the signal
- At the output digital values of the modulated frequency
- Less as possible components
- Take into account future IC designs
- NF lower then 1dB

1.2. STRUCTURE OF THE THESIS

The thesis is organized as follows. In chapter 2 from the requirements given in section 1.1.1 a design for the energy harvesting coil and receiver at system level is discussed. For the energy harvesting coil the different calculation methods are discussed. These calculations will give us an idea what the shape of the coil must be. The backscattered signal from the AWSN is introduced and discussed. Knowing what kind of signal we will receive, the main function blocks of the receiver are presented. Chapter three elaborates on the block diagram of the receiver. Here the blocks are turned into circuitry. Also choices for dedicated IC's needed for the receiver are made and discussed. Simulation results of the coil and receiver circuitry are shown in chapter four. Here the design is verified and compared to the calculated results. The design of the receiver is also verified by measurement in chapter five. Conclusions and recommendations are given in the last part of the thesis.

2

SYSTEM DESIGN

The AWSN is a multiband system. That means that the sensor node uses multiple frequency(RF) channels. In the case of our application there are two frequency channels in two different bands, namely:

- 13.56 MHz for energy harvesting
- 402 MHz for data transmission

For this sensor node we want to design a small antenna for energy harvesting, and a receiver for the information send by the sensor node. This chapter is divided into three main parts. The coil design for the energy link, the calculation of the data link and the system design of the receiver.

2.1. COIL FOR ENERGY HARVESTING

The coil is specified for the AWSN. The coil must comply with the requirements specified in 1.1.1. Calculations which were done are presented in this chapter.

2.1.1. WORKING PRINCIPLE

The IC retrieve his energy via electromagnetic induction. The inductive link consist on 2 coils which are coupled, like a transformer. When there is a varying current through coil 1, an alternating electromagnetic field is produced. Because of the change of flux in the secondary coil, that is produced by the variation of the electromagnetic field, a voltage is induced on coil 2. That phenomenon is also known as Faraday's law:

$$U = -N \frac{d\Phi}{dt} \quad (2.1)$$

Where U is the induced voltage, N the number of turns and Φ the magnetic flux. For properly operation of the IC it is necessary that the impedance of the coil exactly match the conjugate impedance of the IC. Then the transfer of power is maximized, otherwise reflections lead to significant losses. The reflection coefficient is expressed as,

$$\Gamma = \frac{Z_l - Z_s}{Z_l + Z_s} \quad (2.2)$$

Where Z_l and Z_s are the impedance of the coil and the impedance of the IC respectively.

The impedance consists of 2 parts, namely a real part R and a imaginary part X , expressed by:

$$Z_l = R + jX \quad (2.3)$$

Both resistance and reactance are important when determining the coil impedance. The reactance consists of a inductive and capacitive part:

$$X = X_L - X_C \quad (2.4)$$

For both the capacitive and inductive part the reactance is frequency dependent as expressed by:

$$X_L = \omega L$$

and

$$X_C = \frac{1}{\omega C}$$

with

$$\omega = 2\pi f \quad (2.5)$$

The coil capacitance is assumed to be much smaller than the coil inductance, the coil inductance is the most important part of the total reactance. Therefore the total reactance is used to calculate the coils inductance. In [1] the total reactance of the IC is $X_L = -j800$. This means that the coil total inductance has to be $9.348\mu H$ at 13.56 MHz. Given the inductance some calculations have been done to determine:

- Number of turns of the coil
- Shape of the coil
- Trace width
- Trace spacing

2.1.2. COIL CALCULATIONS

In literature [3] [4] [5] [6] different approaches have been found to calculate a coils inductance. It was not obvious which approach was the most accurate. Therefore all approaches have been used to give an overview to examine how many turns are needed for the needed inductance. Used approaches for a circular, rectangle, hexagonal or octagonal shape are stated below. The modified Wheeler has no option for calculating the inductance for a coil. This function is only used for calculating hexagonal shapes. Also some approaches for a rectangle are given.

Melexis approach:

$$L_t = \frac{a^2 n^2}{30a - 11d} \quad (2.6)$$

$$a = \frac{d + n(w + s)}{2} \quad (2.7)$$

Where L_t is the coil inductance, n is the number of turns, w the trace width, s the trace spacing and d is the inner diameter of the coil.

Modified Wheeler approach:

$$L_{mw} = \frac{K_1 \mu_0 n^2 D_{avg}}{1 + K_2 \rho} \quad (2.8)$$

Here L_{mw} is the coil inductance, K_1 and K_2 are some shape dependent parameters, which can be found in [5]. D_{avg} is the average diameter of the coil, μ_0 is the magnetic permeability, and ρ is the fill ratio.

Current Sheet approximation:

$$L_{gmd} = \frac{\mu_0 n^2 D_{avg} C_1}{2} \left[\log \frac{C_2}{\rho} + C_3 p + C_4 \rho^2 \right] \quad (2.9)$$

Here L_{gmd} is the coil inductance, D_{avg} is the average diameter of the coil, μ_0 is the magnetic permeability, and ρ is the fill ratio. The coefficients C_1 to C_4 are shape dependent and can be found in [5].

Used formulas for a rectangle:

Wheeler approach [6]:

$$L_{Wheeler} = \frac{45 \mu_0 n^2 a^2}{22r - 14a} \quad (2.10)$$

$$r = \frac{2(w + h)}{8} \quad (2.11)$$

Here w is the width and h is the height of the rectangle.

$$a = r - \left[\frac{n}{2}(x + s) \right] \quad (2.12)$$

For x is the trace width, n is the number of turns and s is the trace spacing.

Melexis approach:

$$L_T = \frac{n^2 \mu_0}{\pi} \left[-2(w + h) + 2\sqrt{h^2 + w^2} - h \ln \left(\frac{h + \sqrt{h^2 + w^2}}{w} \right) - w \ln \left(\frac{w + \sqrt{h^2 + w^2}}{h} \right) + h \ln \left(\frac{2h}{a} \right) + w \ln \left(\frac{2w}{a} \right) \right] \quad (2.13)$$

Here a is the track width.

The inductance is calculated for a different number of turns. Also by varying the trace width and trace spacing by increasing them with $50\mu m$. That is because of the limit of the local milling machine. The smallest dimension in which the milling machine could make a trace on a FR-4 substrate is $150\mu m$. The maximum sizes of the circular, hexagonal and rectangular shape are stated in table 2.1.

Table 2.1: Used dimensions of different coils

Shape	Length (mm)	Width (mm)
circle	25.75	25.75
hexagonal	25.75	25.75
rectangular	72	19

With the lowest trace width and spacing the highest inductance can be reached. Therefore it is recommended to start the simulations with these dimensions. Also for these dimensions the results are shown below in table 2.2.

Table 2.2: Calculated number of turns for an inductance as close as possible to $9.348\mu H$

Formula	shape	Number of turns	Inductance (H)
Melexis	circle	18	$9.583E-6$
Current Sheet Approximation	circle	18	$9.496E-6$
Current Sheet Approximation	hexagonal	17	$9.251E-6$
Modified Wheeler	hexagonal	15	$9.271E-6$
Melexis	rectangle	7.5	$9.326E-6$
Wheeler	rectangle	8.5	$9.428E-6$

RESISTANCE CALCULATION

Also the series resistance is calculated. But the difficulty is that the resistance consist of two parts. A frequency dependent and a frequency independent part. When an alternating current is flowing through a wire, the current density increases towards the edge of an inductor. That is because of the electromagnetic force, which oppose the current in the middle of an inductor and contributes the current at the edge of the conductor. This is called the skin effect, which is expressed as:

$$\delta = \frac{1}{\sqrt{\pi f \mu \sigma}} \quad (2.14)$$

The skin depth for a frequency of $13.56MHz$ is $0.018mm$. The used copper thickness of the FR-4 laminate substrate is $0.035mm$. The skin depth is smaller then the conductor thickness, what causes an increase in

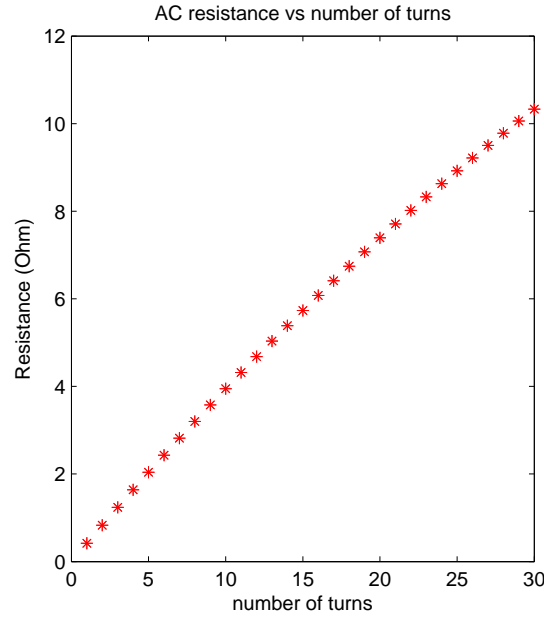


Figure 2.1: Calculated AC resistance for different number of turns and increased trace width and spacing

resistance. But the AC resistance does not depend only on the skin effect. Because the wires in a coil are close to each other another phenomenon occurs, the proximity effect. When for example wires are close to each other and an alternating current is flowing through the wire it will produce an electromagnetic field. This field will produce eddy currents in the nearby wire. And that gives an increase in resistance. An approximated formula for calculating the AC resistance for a conductor etched on dielectric substrate is found in [4]:

$$R_{AC} = \frac{l}{w + t} \sqrt{\frac{\pi f \mu}{\sigma}} \quad (2.15)$$

Where l is the total length of the inductor, w is the trace width and t is the trace thickness. The results for calculating the resistance for the shape of coils from table 4.1 are presented in figure 2.1. Also this is an approximation of the resistance. Because the expression does not include the effects from proximity. Properly calculating the inductance of a coil seems to be difficult. Some reasons for that are:

- The coils behavior is frequency dependent
- Parallel traces give extra capacitance between traces and higher resistance due to the proximity effect

2.2. DATA LINK

As mentioned in chapter 1.1 the AWSN uses backscattering for transmitting the data of the sensor to a receiver. The signal will first be discussed. Afterwards the link budget is calculated to approximate, how much power will be received by the receiver.

2.2.1. RECEIVED SIGNAL

The signal presented in figure 2.2 is the incoming information signal for the receiver. This is the same signal which is also presented in [1]. Note that the received signal is very small, around $\pm 3\text{mV}$.

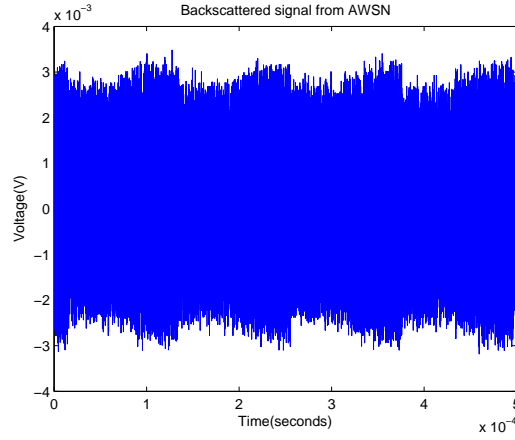


Figure 2.2: Backscattered signal from AWSN node

However this signal is measured direct from the chip in the lab, the actual signal strength will be far less than the current measured signal. The link losses were calculated for the backscattered signal, that means the losses of the transmitted and backscattered signal and the energy absorbed by the AWSN. The used formula is [7]:

$$S = \frac{P_t G_t^2 \sigma \lambda^2}{(4\pi)^3 R^4} \quad (2.16)$$

With σ as:

$$\sigma = \frac{\lambda^2}{4\pi} G^2 \rho^2 \quad (2.17)$$

Used parameters for the formula mentioned above are:

Table 2.3: Parameters used for calculating link losses of backscattered signal

parameter	description	value
S	received signal	
P_t	transmitted energy	-16dBm
G_t	gain of tag antenna	0.5
σ	radar cross section tag antenna	0.0028
λ	wavelength	0.7463
R	distance in meters	0 ... 2 m

The result of the calculated link losses are represented in figure 2.3:

In figure 2.3 the signal strength for a distance of 20cm is -60dB. We also measured the actual link losses. The measurement setup and the measurement itself are discussed in chapter 5.1. The result of the measurements show a link loss around 70dB for 20cm distance. Therefore, a signal power of -80dBm is expected at the input of the receiver.

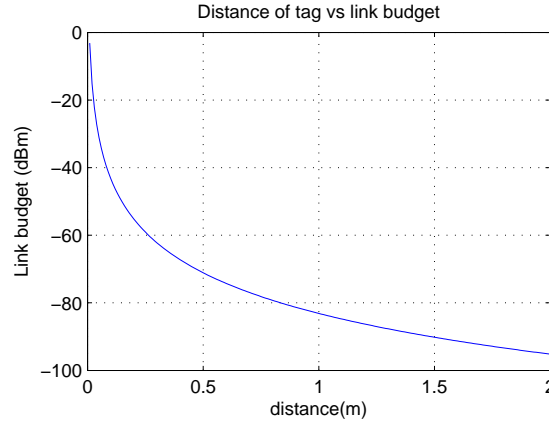


Figure 2.3: Calculated link losses for different distances

2.3. RECEIVER

In figure 2.4 the complete block diagram is shown. The block diagram consist of a low noise amplifier(LNA), a bandpass filter, envelope detector for extracting the information, buffer, low pass filter(LPF), amplifier, averaging circuit for a better accuracy and a comparator.

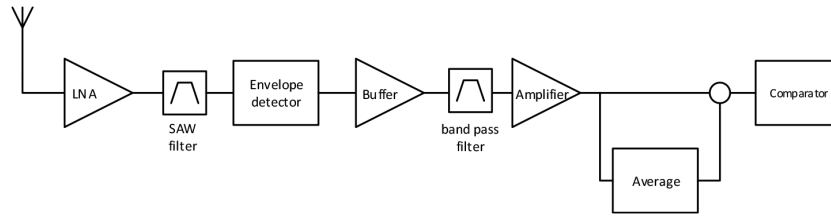


Figure 2.4: Block diagram of receiver circuit

2.3.1. LNA

As presented in the paragraph before, we have to take into account a received signal strength of -80dBm for 20 cm. First we need to amplify the signal before we are able to extract the information. To amplify a received RF signal we made use of an low noise amplifier(LNA). These amplifiers are able to amplify very weak signals and have a very low noise figure. That means that the amplifier itself adds very low noise to the received signal and amplifies the signal with quite high gain. But because the signal we receive is very low we need to cascade LNA with an overall amplification of 60dB. When we use a cascade LNA stage the first LNA is very important, as described by Friis's formula:

$$F_{total} = F_1 + \frac{F_2 - 1}{G_1} + \dots + \frac{F_n - 1}{G_1 G_2 \dots G_{n-1}} \quad (2.18)$$

Where F_n is the noise factor(NF) and G_n is the available power gain of the n-th stage. From this formula you can derive that the first noise factor is dominant for the whole system. Therefore the first amplifier needs a very low NF.

The first block of the system will be a LNA with as low noise as possible. After the first stage some more LNA's are needed depended of the gain of the available LNA's.

2.3.2. BAND-PASS FILTER

When we measured the link losses 5.1 we saw on the spectrum analyzer that close to our band some TV bands are transmitting. Because of the high signal strength of these TV signals we put a bandpass filter. This needs to be a filter with very steep curve to only pass our band and stop all other bands. One simple and very accurate band pass filter is a surface-acoustic-wave(SAW) filter. This filter we will use in order to have a good filtering stage. But because of its relative high NF we put this filter after the first LNA stage.

A SAW filter is needed because of other bands close to our band. Therefore the filter needs a very steep curve. The filter needs to be placed after the first LNA due to NF

2.3.3. ENVELOPE DETECTION

Now the signal is filtered for our band and amplified it is possible to extract the information. Because of the used protocol(OOK) we can use a very simple detector to extract the information. To do this we need an envelope detector.

2.3.4. BUFFER, BAND-PASS FILTER AND AMPLIFIER

After extracting the information of the carrier wave we have to determine when there was a 0 or 1 send. But the received signal of the envelope detector will be very weak, and some RF components will be in the signal. To separate the RF-frontend from the LF-backend we put a buffer between the envelope detector and low frequency(LF) part of the receiver. After the buffer we use a band-pass filter(NF) to remove any residual RF signal components. Through the band-pass filter a clean signal will come in to the amplifier. The signal now is still very small. So we use an amplifier to amplify the signal to a certain voltage level.

2.3.5. AVERAGING AND COMPARATOR

The signal is now clean and amplified. This means that a large enough base-band signal with almost no RF components is coming out of the amplifier. Now we need to find a way to determine the information. The signal actually is still the same that came out of the envelope detector. The idea is to make an average of the amplified signal to have a reference for the comparator. To make an average of the rectified signal a time constant(τ) is introduced. When the time constant of the averaging circuit is much larger then the frequency of the signal an average will be made. Now the comparator have as an input the amplified signal and the average. From these two the comparator is able to make a 0 or 1 of the signal and we have determined the information what is in the received signal.

3

CIRCUIT DESIGN

In this chapter we will have a close look at the receiver block diagram of chapter 2.3. We will discuss the proposed block diagram at circuit level.

3.1. IMPLEMENTATION

The proposed design of the receiver consists of different parts. All of these parts will be discussed in this section. These parts are:

- LNA
- RF filtering
- Envelope detection
- Buffer, base-band filter and amplifier
- Averaging and comparator

3.1.1. LNA

The signal that to be received from the AWSN is very weak as estimated in section 2.2. For the 402MHz band there is no LNA with very high gain and low NF; therefore a cascade of LNA's is required. As the NF needs to be low ($<1\text{dB}$) we chose an LNA with very low NF of about 0.5 dB, namely the HMC616LP3E LNA from Hittite. But this LNA is amplifying all signals that are in the LNA bandwidth. So we don't put the other LNA's after the first one, but first we will filter the signal. Then we put the other LNA's and they only amplifying the signals in our band. In the end we need 3 LNA's to have a total gain of around 60dB. We choose as a first stage(LNA1) the LNA from Hittite because it have a good NF. As a second(LNA2) and third(LNA3) stage we use the LNA from Freescale. That is because the first LNA already have a low NF; therefore the NF of the second and third LNA do not add as much to the overall NF. The LNA2 and the LNA3 are more simpler also.

The specifications of the used LNA's are presented in table 3.1a and table 3.1b:

(a) First LNA specification(by manufacturer)

Hittite	HMC616LP3E	
characteristics	value	unit
Bandwidth	175 - 660	MHz
Gain	21	dB
Noise figure	0.5	dB

(b) Second and third LNA specification(by manufacturer)

Freescale	MBC131916	
characteristics	value	unit
Bandwidth	100 - 2500	MHz
Gain	24	dB
Noise figure	1.07	dB

For the LNA1, the matching network is already specified by the manufacturer. In section 4.2.2 can also be seen that the behaviour of the LNA1 is proper enough for our application. In the datasheet the manufacturer of the LNA2 only specifies a matching network for 900MHz or 1.9GHz. To determine the matching circuit for

the system frequency of 402MHz, we must know the open loop impedance of the the LNA2. To determine the open loop impedance we simulated the LNA2 in an open loop structure in ADS Momentum as can be read in section 4.2.2. The open loop impedance is $73,186 - j102,052\Omega$ for the input and $101,492 - j345,770\Omega$ for the output of the LNA2. Now the matching network need to be calculated. Because if there is no correct match between the input and the LNA2 there will be to much losses. The ideal situation is that both input and output have an impedance of 50Ω .

With the program PASAN, see figure 3.2, the matching network is calculated for the input and output. The open loop impedance is put in the program, and with some components a match is made to 50Ω . For the input it is a capacitor($500pF$) and inductance($40,6nH$) in series. For the output a capacitance($.5pF$) to ground and a series capacitance($14pF$) are needed.

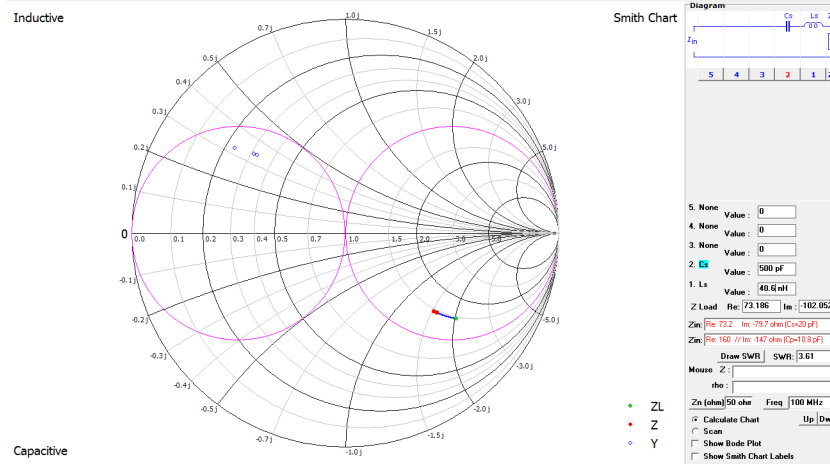


Figure 3.2: Preview of program PASAN

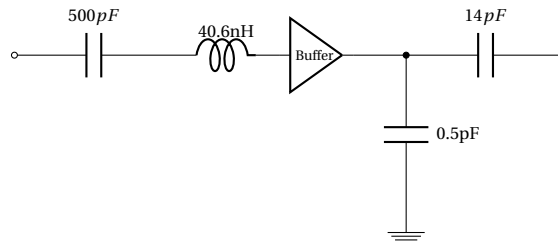


Figure 3.3: Matching network for second LNA

3.1.2. RF FILTERING

The RF filtering will be done with use of a SAW filter. We choose specifically SAW filter from the company Murata. Specifically the RF1419 SAW filter. The specifications of the SAW filter are stated in table 3.1 This SAW filter requires that the input and output is matched to a 50Ω impedance. Thus when designing the PCB we have to consider that. The specifications of the SAW filter are:

Table 3.1: Specification of the SAW filter

characteristics	value	unit
center frequency	403.5	MHz
insertion loss	1.6	dB
bandwidth	7.5	MHz
input/output impedance	50	Ω

Table 3.2: Specification of the envelope detector

Analog Devices	ADL5511	
characteristics	value	unit
bandwidth	DC - 6	GHz
envelope detection bandwidth	130	MHz
minimum input level	-29	dBm

3.1.3. ENVELOPE DETECTION

The detection of an 'envelope' of the transmitted signal in its most simple form, is based on a diode with a capacitor and resistor in parallel. For rectification the signal needs to go above the forward voltage of the diode. But our signal is only a few mV. To have an accurate rectification the forward voltage of the diode has to be around some μVolts . In practice there is no diode with a forward voltage in the order of μVolts . The Schottky diodes have lower forward voltage than common diodes but even these Schottky diodes have no forward voltage of μVolts . Then there are 2 alternatives as a solution:

- Put some extra circuitry to rectify the signal
- Use a IC which has already some circuitry to rectify very small signals

From these options the easiest way is to have an IC that will rectify the signal. We found an IC that is able to rectify small signals. This is an IC from Analog technologies, namely the ADL5511. The specifications of the ADL5511 are stated in table 3.2.

Another positive property of this device is the minimum input level of -29dBm. This means that at the LNA stages we have to amplify to a signal strength a few above -29 dBm. And that will save us the need for an extra LNA. Also this envelope detector has a envelope detection bandwidth of 130 MHz. If in the future more IC's with higher information bandwidths will be produced, the receiver is still capable of extracting the information from the signal.

3.1.4. BUFFER, FILTER AND AMPLIFIER

For both buffer, amplifier and comparator we will use the same opamp, namely the ADA4895-2. For the buffer this amplifier is not really needed but we don't have other amplifiers and this opamp is good enough to operate as a buffer. The choice for the opamp is based on some requirements that the opamp needs to have:

- low off-set voltage ($350\mu\text{V}$)
- High gain bandwidth(GBW)(236MHz)
- low noise ($1\text{nV}/\sqrt{\text{Hz}}$)
- high slew-rate ($943\text{V}/\mu\text{second}$)

The ADA4895-2 meets these requirements. Of course there are opamps which are better at some of the specifications, but this opamp features for all our requirements. The buffer, filtering and amplifying circuit will look like as stated in figure 3.4.

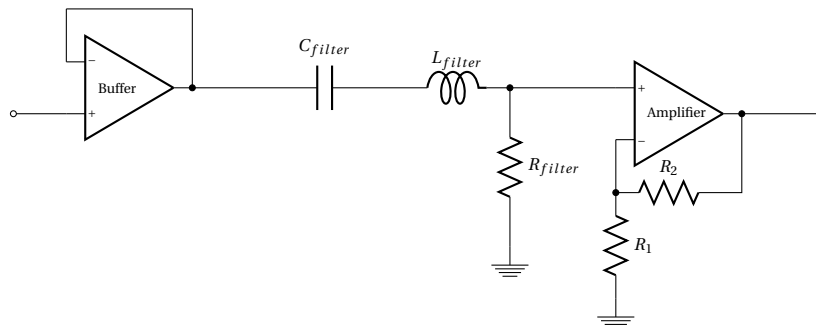


Figure 3.4: LF circuit with buffer, LPF and amplifier

An extra capacitor, C_{filter} is added to decouple the potential DC component in the signal produced by the envelope detector. But this capacitor is also a part of the bandpass filter. We use a bandpass filter because we need to filter quite a wide band and we need a decoupling capacitor. With a normal low pass filter(LPF) we cannot place a capacitor in series, because it will then contribute to the LPE. The frequency of the information has a band from 1kHz till 50kHz. The center frequency of the filter is therefore calculated for a frequency of 25kHz. With the formula:

$$f_c = \frac{1}{2\pi\sqrt{LC}} \quad (3.1)$$

the values of the inductor and resistor were found. The values of the inductor, capacitor and resistor then will be respectively $10\mu H$, $10\mu F$ and 15Ω .

The amplifier is a normal non-inverting amplifier. The resistors R_1 and R_2 form a feedback to the amplifier and with them we can define the gain. The formula is:

$$V_{out} = V_{in} \left(1 + \frac{R_2}{R_1}\right) \quad (3.2)$$

Where V_{in} is the signal from the band-pass filter. The signal from the filter will be still small around some mV . The off-set voltage of the comparator is $350\mu V$. To have an accurate comparison we want to have a high gain to have a larger signal to noise ratio. We choose for a gain of 10. Then the signal should have an amplitude around $30mV$. The values of the resistors R_1 and R_2 are then $10k\Omega$ and $1k\Omega$ respectively.

3.1.5. AVERAGING

The low pass filter has a time constant because of the capacitor. An low pass filter is very easy to implement and work fine for our application. Therefore we will use a cascade of two low pass filters as an averaging circuit as can be seen in figure 3.5.

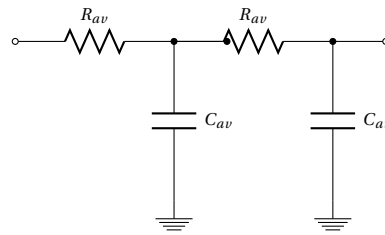


Figure 3.5: Averaging circuit

The time constant can be calculated with formula:

$$\tau = RC = \frac{1}{2\pi f_c} \quad (3.3)$$

Where τ is the time constant, and f_c the cut-off frequency. For our application the cut-off frequency is set to 500Hz. Then the values for the resistor and capacitor are respectively 330Ω and $1\mu F$.

3.1.6. COMPARATOR

The receiver has to determine if there was a 0 or 1 send by the AWSN. If the envelope and averaging are working correctly then it would not be that difficult to determine a 0 or 1. The detection is done with a comparator. It is an opamp with no feedback. At the negative input there is the reference voltage, which comes from the averaging and at the positive input the extracted signal. The comparator will look as illustrated in figure 3.6.

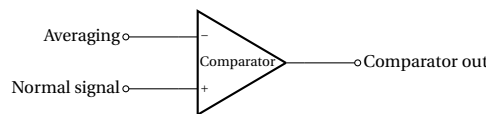


Figure 3.6: Comparator circuit

3.2. CONCLUSION

Now we have discussed the whole circuit. The different parts are discussed and choice for the specific IC's have been argued. The values for the resistors etc. are discussed in the next chapter Circuit simulation.

3.2.1. COMPLETE CIRCUIT

After all the different circuitry parts we discussed the complete circuit is presented in figure 3.7.

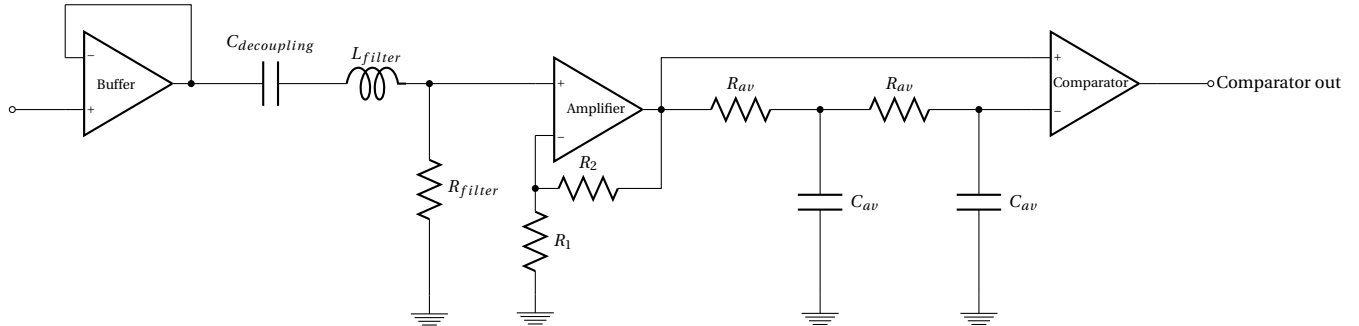


Figure 3.7: Complete proposed LF circuit

4

CIRCUIT SIMULATION

The simulation of the energy harvesting coil and the receiver circuitry are discussed in this chapter. To verify the designs that are proposed, they are simulated. First the coil is simulated and then the receiver.

4.1. COIL SIMULATION

The deviations in the calculated number of turns to reach an inductance of $9.348\mu H$ in chapter [Coil calculations](#) are quite big. Therefore another method is used to check the equations. The coil is modeled in a simulation program called ADS Momentum. This is a 2.5-D simulation program which calculates the coils inductance by use of differential equations. The total results of different coil shapes, trace width and trace spacing are described in appendix [Coil Simulation and Calculation results](#). The final design will be a hexagonal shape for the coin shaped coil. This shape is chosen because a higher resistance can be achieved when the corners in a coil are more sharpened. That is also determined from the simulation results. As stated in formula [2.3](#) and [2.2](#) it is important to achieve a resistance that is the same as the resistance of the IC.

The number of turns, trace width and trace spacing which were determined by simulation for both the coin shape and bandage shape are shown in table [4.1](#).

Shape	Number of turns	Trace width (mm)	Trace spacing (mm)	Inductance (H)	Resistance (ohm)
hexagonal	18	0.15	0.16	9.05E-6	7.21
rectangle	8.5	0.15	0.16	9.08E-6	10.47

Table 4.1: Derived simulation results for hexagonal and rectangular coil

From the simulations in ADS Momentum we can derive that the equations do not exactly match with the simulations. All of the equations have some deviation. That is also not so strange because not all of the parasitics that occur are taken into account when calculating the coils. But for a first approximation they are useful. For a final design, we have to rely on an electromagnetic simulation.

4.2. RECEIVER SIMULATIONS

The simulations were divided in three parts. One is the RF frontend of the receiver in simulink to verify the block diagram of the receiver blocks. This is a very early simulation of the proposed receiver network. The second part is the RF-frontend simulated at circuit level, third the LF backend is simulated. The RF circuit simulations for the LNA's and SAW filter were done with ADS Momentum. The envelope detector cannot be simulated. The operation of this device can only be determined by measuring. The LF-backend circuit simulations were done with LTSpice. This is a free SPICE simulator from Linear technology in which one can use 3rd party models. The ability of using 3rd party models makes this simulator very suitable for our simulations. The buffer, filtering, amplification, averaging and the comparator stage were simulated with LTSpice.

For the RF simulations in ADS we used the S-parameters provided by the manufacturer for the LNA's and the SAW filter.

4.2.1. SIMULINK

In Matlab Simulink the complete RF front-end is simulated. This simulation with Simulink is to satisfy our thoughts about the RF receiver topology. This simulation therefore is a high level simulation. No parasitics are included. For this reason the SAW filter is also not included. As an input signal we used the provided signal as presented in section 2.2. The simulations were done with ideal components. Goal is to extract the transmitted signal without any HF components in it.

An other thing that has to be determined in simulation is the rectifying stage. Because we already know that the signal is very small, and there is no diode with a V_f of some μV . But this should be possible with the proposed IC. So a simple model is made of the IC to simulate the behaviour and to determine the working of the IC and receiver topology.

The Simulink model can be seen in figure 4.1. The results are presented in figure 4.2 and 4.3.

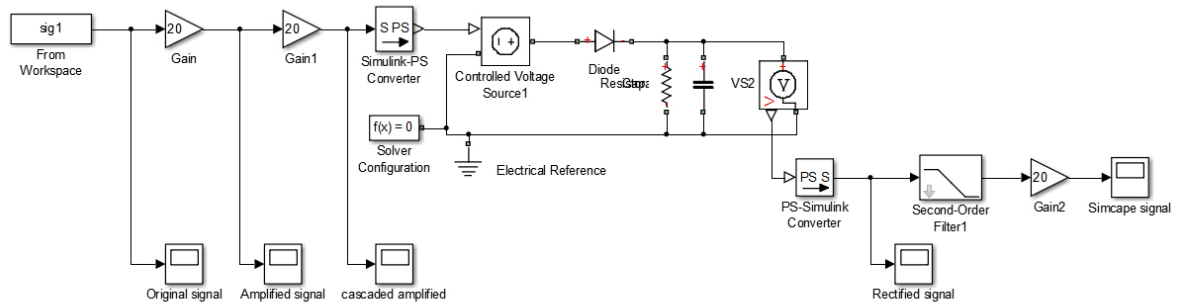
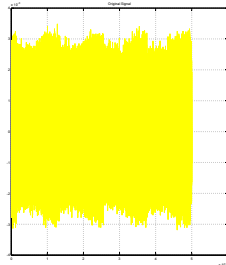


Figure 4.1: Matlab Simulink model of proposed receiver design



(a) Input signal from AWSN



(b) Amplified signal

Figure 4.2: Simulink simulation results



Figure 4.3: Simulink simulation results

The simulation results show a good result of the proposed topology of the front-end receiver. With a very low V_f of the diode the rectifying looks correct. This have to be verified by measurement of the rectifier IC. Because there is no S-parameter file of this chip, or PSPICE model. The signal strength at the end of the RF front-end is really big, about 20Volts. But due to losses and even more a very weak input signal this will be far more less.

4.2.2. RF-FRONTEND SIMULATIONS

In ADS we simulated the matching circuits for the first LNA and the second LNA and the SAW filters.

LNA1

The LNA1 is provided with a matching network and from that circuit the S-parameters are available from the manufacturer. With these parameters we did a simulation to see how the devices behaves at our frequency. In figure 4.4 the S-parameters of the LNA1 are shown.

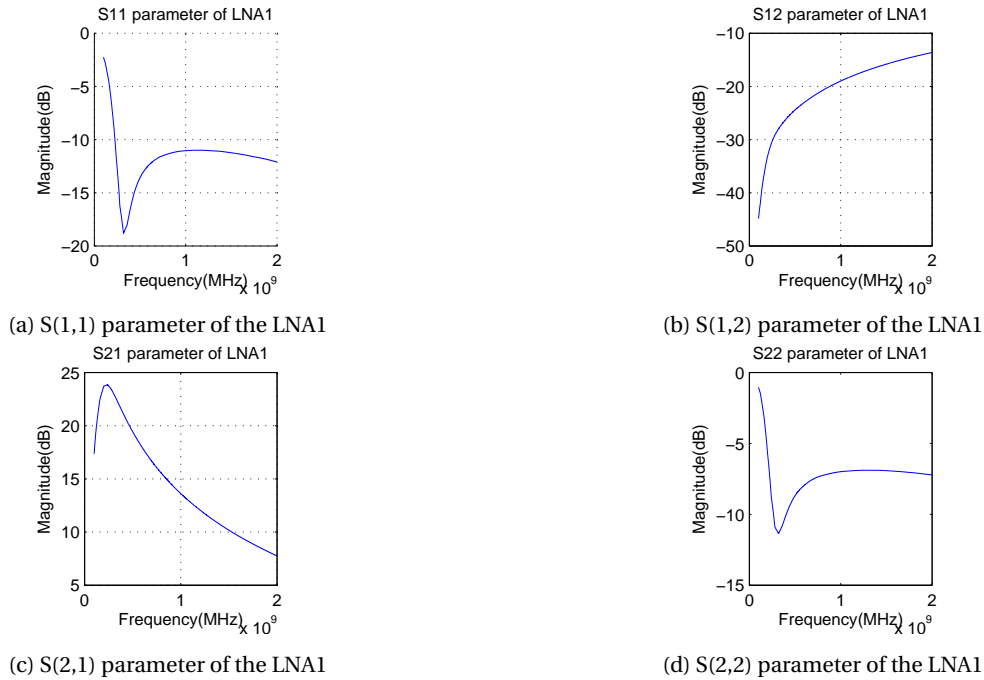


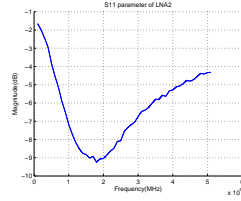
Figure 4.4: S(1,1), S(1,2), S(2,1) and S(2,2) of the LNA1 with matching network

In figure 4.4 to see is that the operation of the LNA1 should be good in our band. The reflection at the input of the device is less, as can be seen by the S(1,1) and S(2,2) parameters. That means that there are few losses at the input. The The gain of the LNA1(S(2,1)) is decreasing when going towards 1GHz, but at our band it

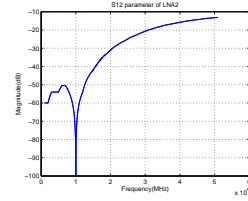
still have a gain of 20dB. At least a gain of around 20dB is required and therefore we do not have to make a modification to the matching network.

LNA2 AND LNA3

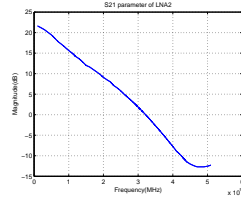
The network with the matching elements is also simulated. First the LNA2 without any matching is simulated to have the open loop impedance of the LNA2. With the open loop impedance we can derive the correct matching network. The open loop simulation is shown in figure 4.5. The proposed matching network is placed in ADS and with the by manufacturer provided S-parameters we simulated the behavior of LNA2.



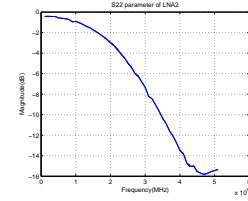
(a) S(1,1) parameter of the LNA2



(b) S(1,2) parameter of the LNA2



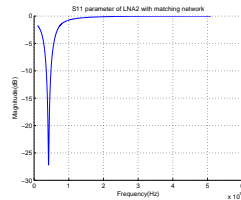
(c) S(2,1) parameter of the LNA2



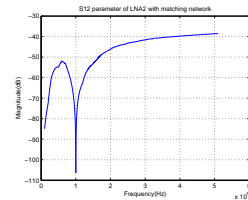
(d) S(2,2) parameter of the LNA2

Figure 4.5: S(1,1), S(1,2), S(2,1) and S(2,2) of the LNA2 with matching network

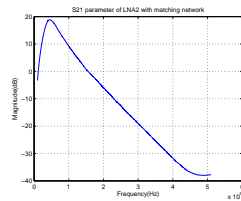
In figure 4.6 one can see that the circuit is now well matched. The real part of $Z(1,1)$ and $Z(2,2)$ are close to 50Ω . And the imaginary part of $Z(1,1)$ and $Z(2,2)$ are close to zero. The $S(1,1)$ is at 400MHz almost -20dB which is very good. The overall gain of the complete network is a little bit decreased. That occurred through the extra components needed for matching. These components consume some power, but it is very little (2dB).



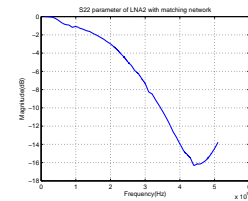
(a) S(1,1) parameter of the LNA2 with matching network



(b) S(1,2) parameter of the LNA2 with matching network



(c) S(2,1) parameter of the LNA2 with matching network

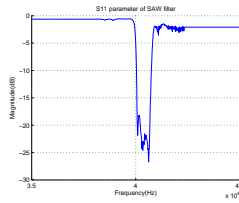


(d) S(2,2) parameter of the LNA2 with matching network

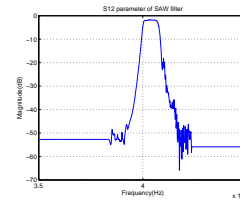
Figure 4.6: S(1,1), S(1,2), S(2,1) and S(2,2) of the LNA2 with matching network

SAW FILTER

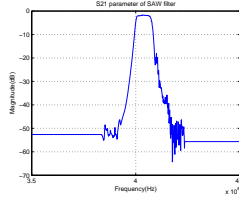
The behavior of the matching network of the SAW filter is simulated in ADS. The network is terminated with 50Ω input and output terminals. The results of the simulation are shown in figure 4.7.



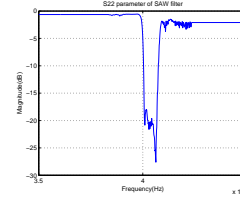
(a) S(1,1) parameter of the SAW filter



(b) S(1,2) parameter of the SAW filter



(c) S(2,1) parameter of the SAW filter



(d) S(2,2) parameter of the SAW filter

Figure 4.7: S(1,1), S(1,2), S(2,1) and S(2,2) of the SAW filter

To see in the graphs is that the S(1,1) and S(2,2) parameters are quite good. Both are below -10dB what means that there is little reflection at the input and output of the SAW filter. The input impedance is almost near to 50Ω , what makes the input very well matched. The output is little unmatched. The insertion loss of the SAW filter is close to 6dB. This is still below what is described in the datasheet so we may expect a working SAW filter.

4.2.3. LF-BACKEND SIMULATIONS

In LTspice we verified the behaviour of the LF-backend circuit. For the opamp in the simulations we used the SPICE model of the ADA-4895 opamp. That is the opamp we already discussed in 3.1.4. As an input signal, we choose for the measured signal from the envelope detector at a frequency of 50kHz. The measurement can be found in 5.5.1. The input signal is shown in figure 4.12. At the end of the graph the signal goes to 0V. This is caused by the input file of the simulation program.

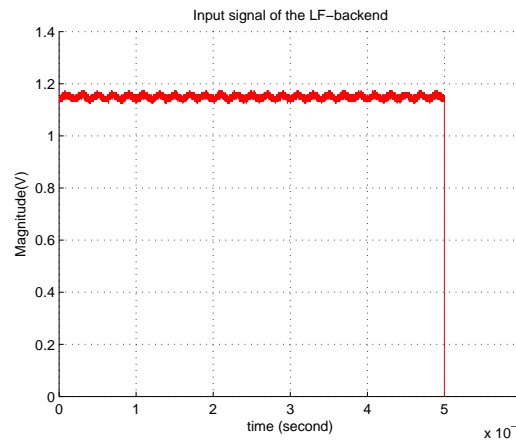


Figure 4.8: Inputsignal of the LF-backend

4.2.4. BUFFER

As a buffer we chose the ADA4895, as said in 3.1.4. But when simulating with the SPICE model of the ADA4895 the simulation time is too long. Therefore the buffer is simulated only. The result is shown in figure 4.9.

To see is that this opamp is not suitable for use as a buffer. There will have to be looked to another opamp which is suitable as a buffer. But this one is distorting the signal.

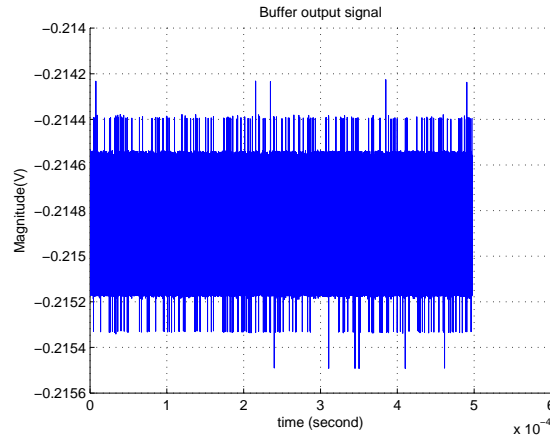


Figure 4.9: Output signal of buffer

4.2.5. FILTER

The behaviour of the filter should be good when looking to the filter characteristics in figure 4.10. To see is that the left -3dB point of the filter is at 1kHz which is the lowest frequency of our band. The right -3dB point of our filter is at 250kHz. That is good enough because it filtered out the remaining RF frequencies. And the attenuation of the DC components should also be enough.

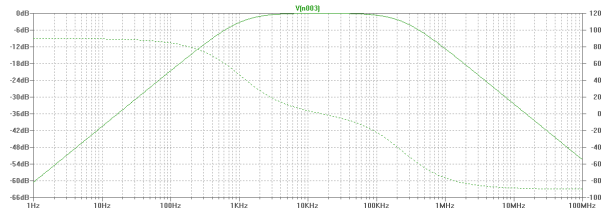


Figure 4.10: Filter characteristics of the LF filter

That the filter is working properly is also seen in the simulation results when the filter is simulated with the input signal, mentioned in 4.2.3. That is to see in figure 4.11. The DC component is filtered out by the series capacitor, as can be seen that the signal is around 0V. The remaining RF frequencies are also filtered out by the filter. The signal

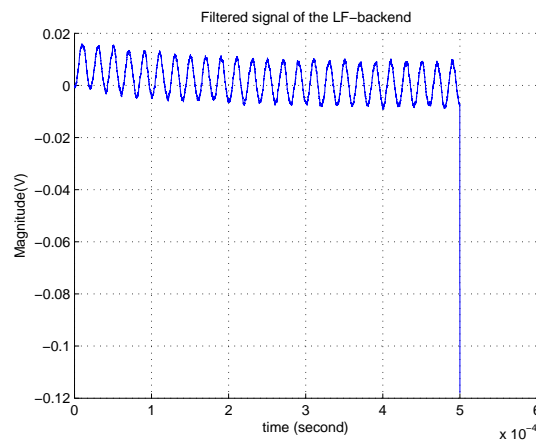


Figure 4.11: Input signal of the LF-backend

4.2.6. AMPLIFIER

When looking at the amplifier we see that in the simulation it is amplifying well. The signal is a little bit shifted but that is due to the offset of the amplifier.

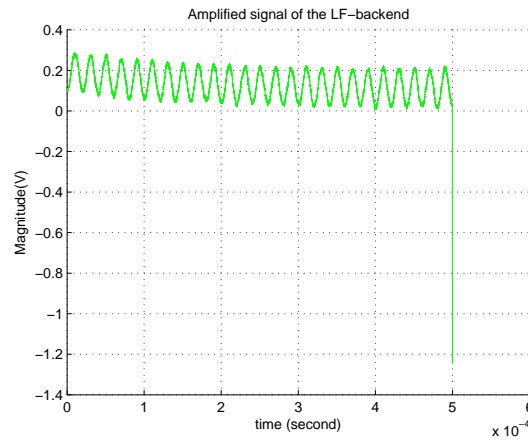
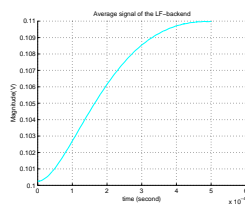


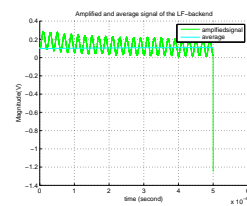
Figure 4.12: Inputsignal of the LF-backend

4.2.7. AVERAGING

With the averaging circuit we want to have as flat as possible average of the signal. In figure 4.13b it is to see that an almost flat average is made. There is a settling time, because of the capacitors in the averaging circuit. That is seen more clear in figure 4.13a.



(a) Settling curve of the averaging circuit



(b) Average and amplified signal before comparator

4.2.8. COMPARATOR

The input of the comparator is shown in figure 4.13b. From this input the comparator is supposed to make a square wave. In figure 4.14 it is to see that a square wave is made. Also it has a duty-cycle of around 50%. In the beginning the average is not settled and therefore the comparator is not working correct at that time. But later on it does, and is very stable. The square wave itself looks also good. the ramp are very steep, and amplified till the input voltages of the comparator.

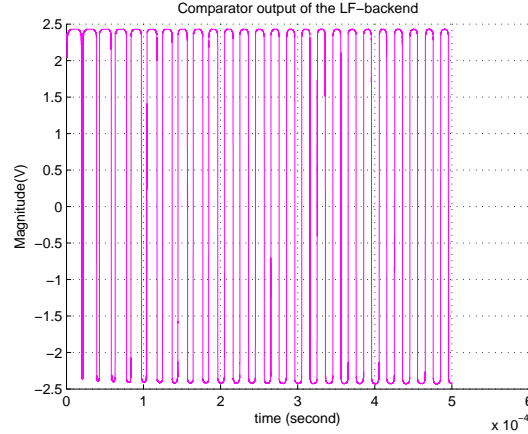


Figure 4.14: Comparator output of the LF-backend

4.2.9. COMPLETE LF-BACKEND

The complete LF-backend behaviour is drawn in figure 4.15.

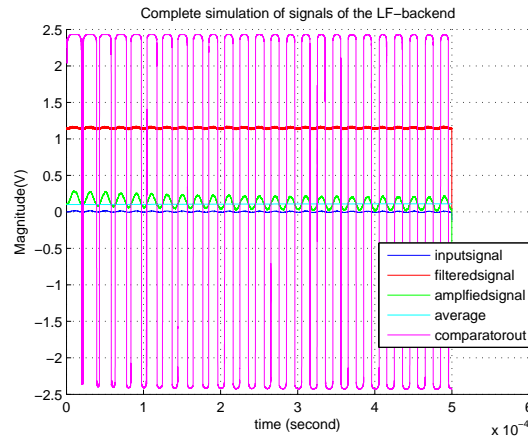


Figure 4.15: Inputsignal of the LF-backend

5

MEASUREMENTS

In this chapter all measurements that have been done are presented. For all measurements first the measurement setup is given then the measurement results. The coil for energy harvesting is not measured. Because the milling machine is not able to manufacture the coil, the coils could not be measured. Also a complete test of the whole receiver, as a test of the whole receiver with the antenna's as a test of the receiver with the AWSN is missing due to lack of time.

5.1. LINK LOSSES

The link losses were measured to determine the link losses in air. As calculated the link losses should be around 30dB for only one link. Complete link losses for one transmission are then 60dB. The link losses were measured in the lab. Therefore 2 PCB's have been made with both an antenna. The specifications of the antenna are stated in table 5.1 and the measurement setup is shown in figure 5.1.

Table 5.1: Characteristics of used antenna for measuring link losses

characteristic	value	unit
working frequency	400-500	MHz
Gain	0.5	dBi
Polarization	linear	
Impedance	50	Ω

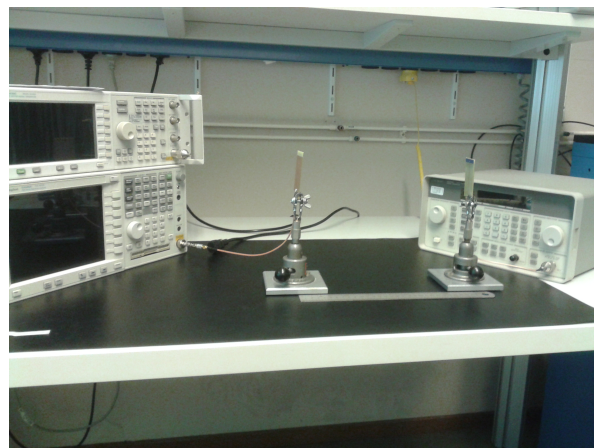


Figure 5.1: Measurement setup for measuring the signal losses in air

In figure 5.2 the the used devices are:

Table 5.2: Measurement setup link losses

Device	settings
Agilent 8648C signal generator	402 MHz AM signal
Agilent E4446A network analyzer	measuring between 390MHz – 415MHz

MEASUREMENT RESULTS LINK LOSSES

Figure 5.2 represents the measurement results. One can see that the peak of the transmitted signal is exactly at 402MHz. The signal losses for only one link are, when sending with 0dBm, 31.79dB at a distance of 30cm. That means that the total loss of transmitted signal is $2 * 31.79 = 63.58dB$. The consumed energy of the AWSN will be around 6dB. Total attenuation of the signal will be around 70dB.

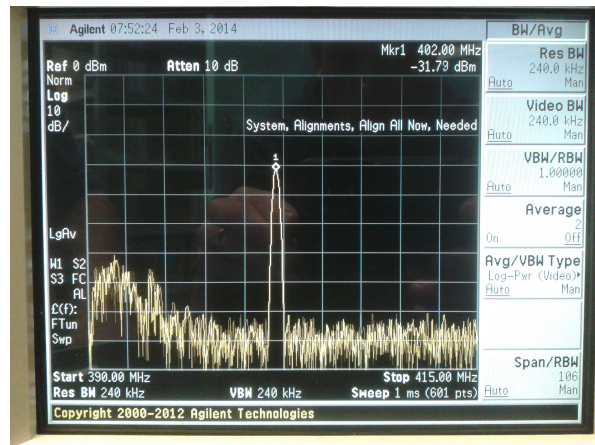


Figure 5.2: Measurement result of received signal signal

5.2. LNA's

To verify the correct behaviour of the three LNA's we measured them. The measurement setup for the components is stated in table 5.3. The LNA's are measured with use of S-parameters. The output power of the VNA is -13dBm.

Table 5.3: Measurement setup LNA

Device	type	settings
Agilent 8753E	Vector network analyzer	350MHz..450MHz @-13dBm
Agilent 85047A	S-parameter test set	
Delta elektronika D 030-1	power source	4.5V

MEASUREMENT RESULTS LNA1

In figure 5.3 the measurement results of LNA1 is shown. In table 5.4 the simulated and measured values are stated to have an idea of the deviations.

Table 5.4: Comparison between simulation and measured S-parameters LNA1

S-parameter	simulated(dB)	measured(dB)
S11	-16.280	-17.607
S21	21.176	20.598
S12	-26.187	-25.164
S22	-10.075	-16.014

In table 5.4 the simulated and measured values for different S-parameters are stated. Most of the values are quite the same. The small deviations are due to some losses in trace lines or less soldered components. But

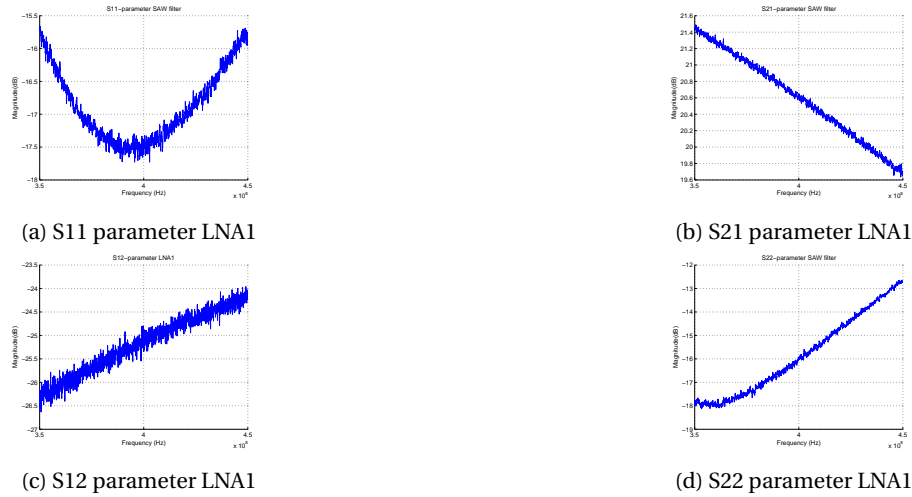


Figure 5.3: S-parameters LNA1

these losses are acceptable because we still have a gain of 20dB and good results of $S(1,1)$ and $S(2,2)$ which are below -10dB. The big difference between the simulated and measured value in $S(2,2)$ is strange. Probably it is due to the PCB we made. We made it some smaller then the one that the manufacturer described. But a $S(2,2)$ of -16dB is very good.

MEASUREMENT RESULTS LNA2 AND LNA3

In figure 5.4 and figure 5.5 the measurement results of respectively LNA2 and LNA3 are shown. In table 5.5 the simulated and measured values are stated to have an idea of the deviations.

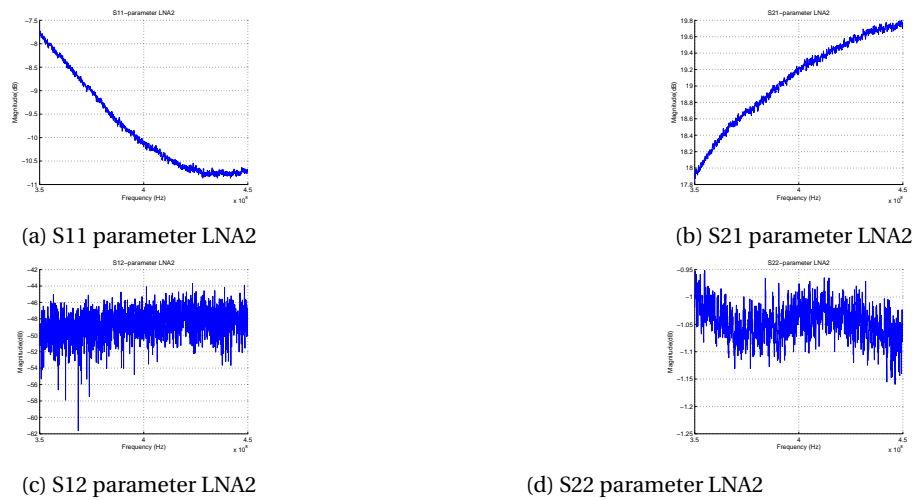


Figure 5.4: S-parameters LNA2 without matching network

Table 5.5: Comparison between simulation and measured S-parameters LNA2 and LNA3

S-parameter	simulated(dB)	measured LNA2(dB)	measured LNA3(dB)
S11	-20.765	-10.182	-8.072
S21	18.477	19.277	19.518
S12	-55.559	-48.122	-38.391
S22	-0.184	-1.0251	-5.616

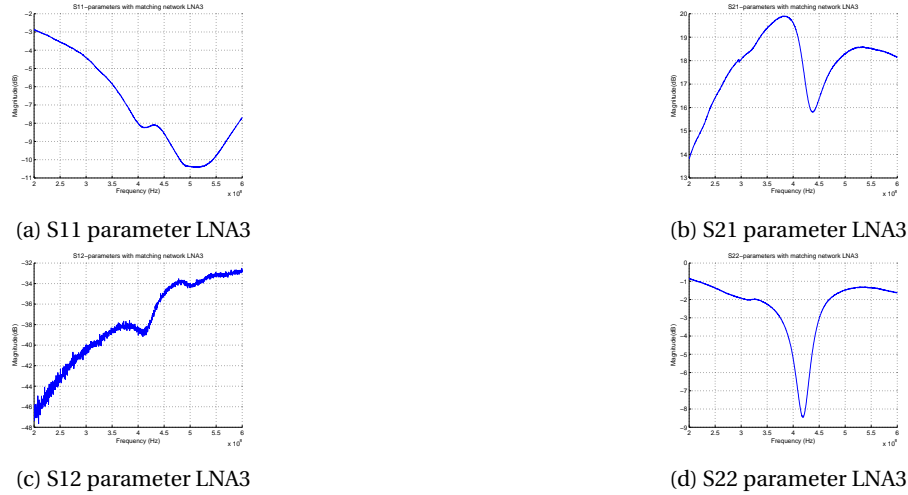


Figure 5.5: S-parameters LNA3 with matching network

5.3. SAW FILTER

Also the SAW filter is measured. Since the SAW filter is an passive device we only use the VNA to measure the behaviour of the SAW filter. We want to know how the filter respond to different frequencies. We measured from 350MHz till 450MHz. With the measurement we want to see how the filter will behave when mounted on the PCB. The filter don't need an matching network, but the trace lines of the PCB may provide a bit of induction to the input of the SAW filter. The used devices we used for the measurement are stated in table 5.6.

Table 5.6: Measurement setup SAW filter

Device	type
Agilent 8753E	Vector network analyzer
Agilent 85047A	S-parameter test set

MEASUREMENT RESULTS SAW FILTER

Below in figure 5.6 the measurement results of the SAW are plotted. The actual simulated and measured values for the different S-parameters are stated in table 5.7. To see in figure 5.6b the response is very good. There is less insertion loss then the maximum specified loss in the datasheet(2.5dB). The input losses are a bit higher. That is due to less matching. Because a SAW filter is very sensitive to it's input impedance the losses will increase with only a little mismatch. The input losses are still quite good so there is no need to redesign this.

Table 5.7: Comparison between simulation and measured S-parameters SAW filter

S-parameter	simulated(dB)	measured(dB)
S11	-18.857	-11.438
S21	-1.978	-2.1916
S12	-1.972	-2.2472
S22	-18.580	-12.483

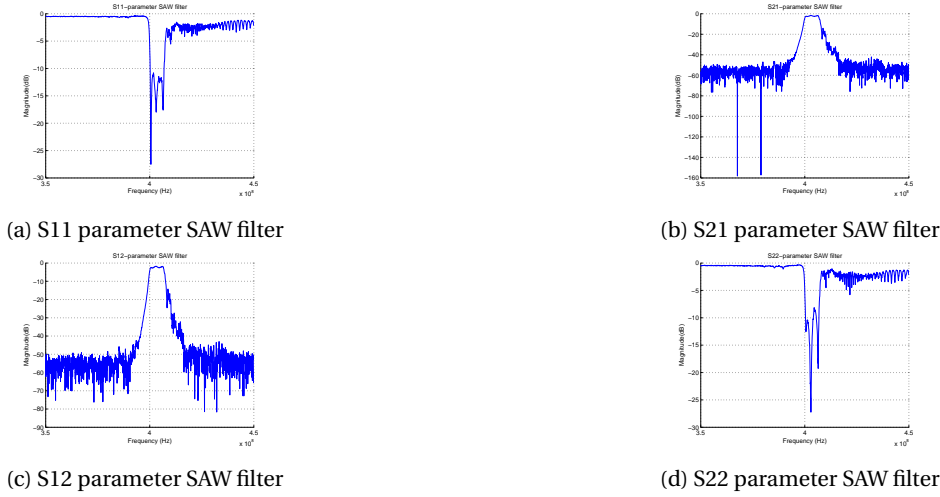


Figure 5.6: S-parameters SAW filter

MEASUREMENT LNA1, SAW FILTER, AND LNA2

Also we made an measurement with LNA1, the SAW filter and LNA2 to have an idea of the behaviour of the whole RF-frontend. LNA3 is not included in this measurement, because it was not mounted on the time we did this measurement. LNA3 only amplifies the signal more but the contribution will be quite the same as LNA2. That is also seen in paragraph 5.2. The RF-frontend is measured with 20dB attenuation in the VNA because of the 1dB compression point of LNA2 (-5dBm input power). Because there is such a high gain the total amplification will be above 0dBm and the LNA2 cannot deliver that amount of power. The results are stated in figure 5.7

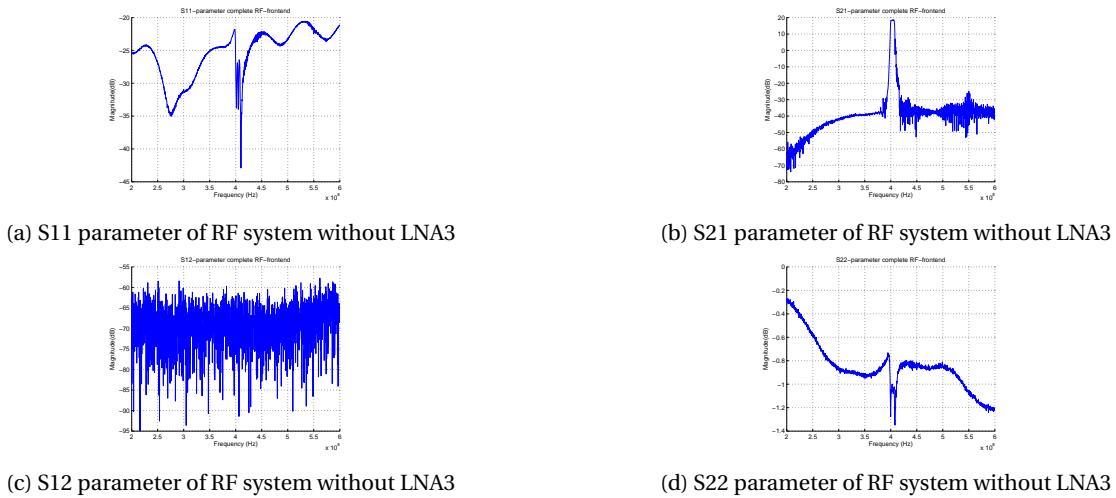


Figure 5.7: S-parameters of measurement of LNA1, SAW filter, and LNA2

The graphs shows a behaviour of the two LNA's and SAW filter like we expected. The gain($S(2,1)$) is 18dB what means in fact that it is 18dB+20dB attenuation = 38dB of total gain. The $S(1,1)$ is very good, and so is the $S(1,2)$. The $S(2,2)$ is also a little bit increased but not that good. But with the parameters of LNA3 we may assume that there will be a little increase in $S(2,2)$ when LNA3 is connected to the RF-frontend.

5.4. RF FRONT-END NOISE FIGURE AND GAIN

The influence of the LNA's and SAW filter in the RF-frontend is indicated with the noise figure parameter. As already said in chapter 1.1.1 the NF should be below 1dB. That means that there is very less noise embedded in the RF signal, which also will be a sort of noisy because of the weakness of the received signal. For this measurement the devices we used are stated in table 5.8.

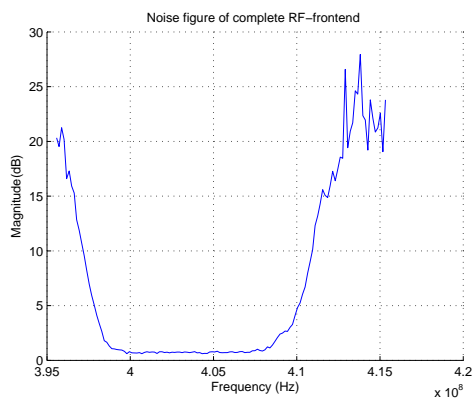
Table 5.8: Measurement setup RF front-end

Device	type	
Agilent N8973A	Noise figure analyzer	
HP 346A	Noise source 10MHz–18GHz	
Delta elektronika D 030–1	power source	4.5V

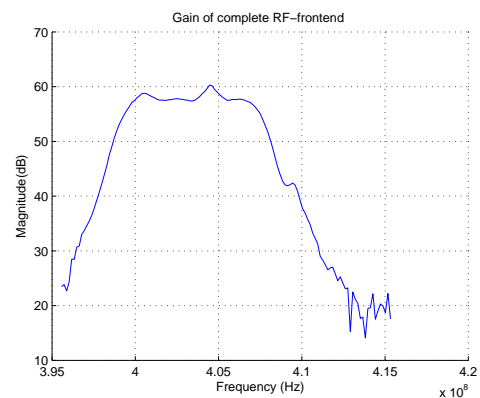
The results of the NF measurement, shown in figure 5.8, are very good. The overall NF of the complete RF-frontend is below 1dB. In fact it is 0.891dB. Actually this is quite high compared to the NF of the first LNA which should be 0.5dB. Why this can be so high is a little strange. But the little mismatch at the input of the SAW filter good be a reason for it.

As we expected the gain is around 57dB. All LNA's have a gain of around 19dB, and with 3 cascaded LNA's it should be around 57dB. To see in figure 5.8b is that the gain is also quite stable in our band. There is a peak around 404MHz, but the bandwidth of the AWSN is only 50kHz, so we won't see any difference in gain.

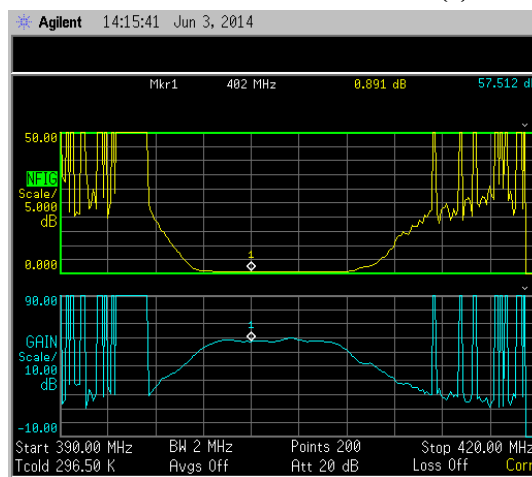
The strange peaks in figure 5.8c are in the band that is filtered out by the SAW filter. Because the signal is so low in this band that all kind of strange signals will appear. But to see is that for our band the NF and gain are quite good.



(a) Noise figure of complete RF frontend



(b) Gain of complete RF frontend



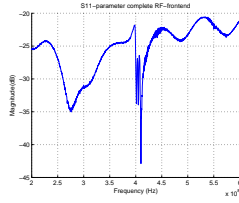
(c) Picture of Noise figure analyzer when measuring the noise figure and gain of the whole RF frontend

Figure 5.8: NF and gain plots from receiver

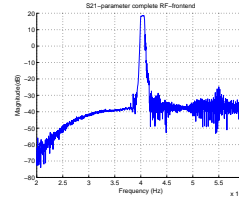
MEASUREMENT LNA1, SAW FILTER, AND LNA2

Also we made an measurement with LNA1, the SAW filter and LNA2 to have an idea of the behaviour of the whole RF-frontend. LNA3 is not included in this measurement, because it was not mounted on the time we

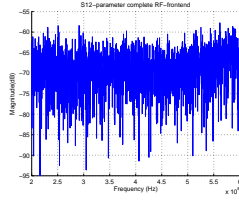
did this measurement. LNA3 only amplifies the signal more but the contribution will be quite the same as LNA2. That is also seen in paragraph 5.2. The RF-frontend is measured with 20dB attenuation in the VNA because of the 1dB compression point of LNA2(-5dBm input power). Because there is such a high gain the total amplification will be above 0dBm and the LNA2 cannot deliver that amount of power.



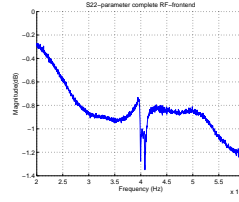
(a) S11 parameter of complete RF system



(b) S21 parameter of complete RF system



(c) S12 parameter of complete RF system



(d) S22 parameter of complete RF system

The graphs show a behaviour of the two LNA's and SAW filter like we expected. The gain(S(2,1)) is 18dB what means in fact that it is 18dB+20dB attenuation = 38dB of total gain. The S(1,1) is very good, and so is the S(1,2). The S(2,2) is also a little bit increased but not that good. But with the parameters of LNA3 we may assume that there will be a little increase in S(2,2) when LNA3 is connected to the RF-frontend.

5.5. MEASUREMENT SETUP ENVELOPE DETECTOR

For the envelope detector we ordered a complete evaluation board with the IC we needed already mounted on it. First we tested only the envelope detector on how it will behave with a sine AM wave. After this measurement the envelope detector is tested with the complete RF-frontend. For the first measurement we used an AM modulated signal, with a carrier frequency of 402MHz and a data signal of 500kHz. The 500kHz was to test the envelope for a higher bandwidth needed in the future for an AWSN with ECG. The second measurement was made with the complete RF-frontend. Here an AM modulated signal, with a carrier frequency of 402MHz and a data signal of 50kHz is used. The modulation depth is 30%.

The first measurement setup with a sine AM wave is done with the devices stated in table 5.9. For the measurement with the whole RF-frontend we didn't use the waveform generator, and we use a different power supply, namely the Delta elektronika D 030-1.

Table 5.9: Measurement setup envelope detector

Device	type
Agilent InfiniVision DSO-X 3032A	oscilloscope
Agilent 33500B	waveform generator
Agilent E4438C	vector signal generator
Keithly 6430	source meter

5.5.1. ENVELOPE DETECTOR

The measurement of the envelope detector was straight forward. To see in figure 5.10 the signal is very clean. Yet the signal has an offset of 1V, but that is compensated in the filter at the LF-backend. In figure 5.11 the signal from the measurement of the whole RF-frontend is shown. The input signal for this measurement was -85dBm with an modulation depth of 30%. That means that the RF-frontend now is capable of detecting a signal that is reaching the requirements. The signal from the envelope detector looks a little bit noisy. But that is due to quantization noise from the oscilloscope. On the oscilloscope the signal looks very good but unfortunately we don't have a picture of that. But to see is that the envelope is detected, and that the signal looks quite well.

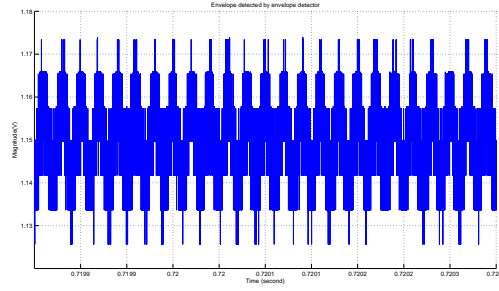


Figure 5.10: Envelope(50kHz) detected by envelope detector only

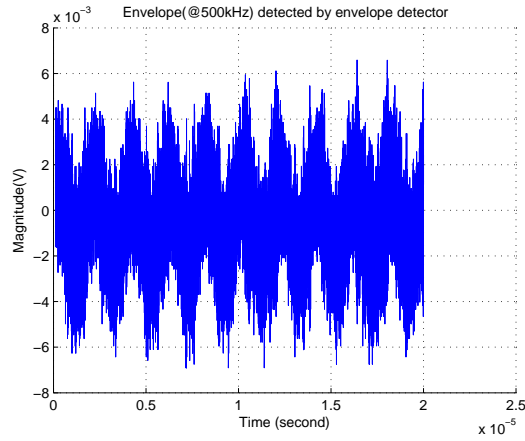


Figure 5.11: Envelope(500kHz) detected by envelope detector with whole RF-frontend

5.6. LF-BACKEND

Now the whole RF-frontend is measured and works, we can start measuring the LF-backend. This is done first with measuring only the LF-backend and as an input a signal of 50kHz and a magnitude of 10mVpp. The LF-backend is powered up by a pair of batteries. These batteries are 1.5V each and connected in series to have a ± 1.5 power supply. The devices we used for this measurement are stated in table 5.10.

Table 5.10: Measurement setup LF-backend

Device	type
Agilent InfiniiVision DSO-X 3032A	oscilloscope
Agilent 33500B	waveform generator
Delta elektronika D 030-1	power source

Measurement results LF-backend Before we actually started with measuring the LF-backend we found out that there is a signal interfering with our measurements. This interfering signal causes a lot of noise on our input signal and therefore it was hard to have a good measurement. In figure 5.12 the interfering signal is shown. It can be seen that the input signal is very noisy and that the frequency of the noise is around 90MHz. Because of the interfering signal we used batteries with short wires to have as less as possible noise from the power supply. Despite of the noise that is in our signal we made some measurements to verify the operation of the circuit.



(a) LF backend input signal with lot of noise on it

(b) Determined noise frequency on the input signal

Figure 5.12: Input signal for LF backend with noise and determined frequency of the noise

Measurement results buffer The correct behaviour of the buffer is little uncertain. Even though the rest of the circuit seems to work quite well, the signal that comes from the buffer is very strange. There is noise in the signal but the buffer should only buffer the signal and now there is a lot of noise added. It could be because of high frequency of the noise and the gain bandwidth product of the amplifier, but that we are not sure. And that is difficult to test since we can not get off the noise.

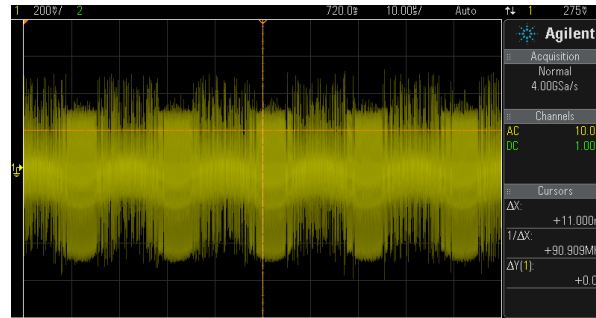


Figure 5.13: Signal that is coming out of the buffer in the LF-backend

Measurement results filter Even though the buffer produces a strange output, the filter seems to work quite well. Still there is a little bit of noise and some glitches occur, see figure 5.14, probably due to the buffer output. It remains difficult to say how well the filter behaves due to the noise. But the signal which is filtered have the correct frequency, so that might indicate that the filter is working properly.

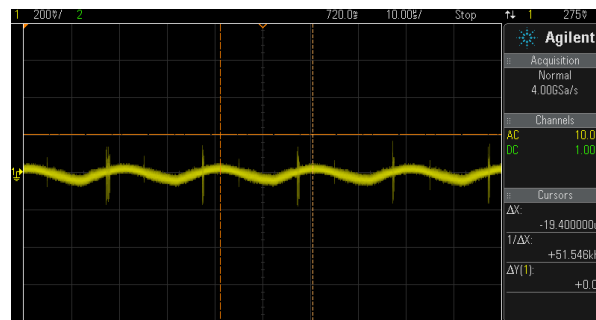


Figure 5.14: Filtered signal before amplifier in the LF-backend

Measurement results amplifier and averaging We know the signal form the filter and when looking at the signal that is coming out of the amplifier we may conclude that the amplifier is working. The amplifier has a gain of 10 and we can see that also in figure 5.15, remaining that the signal in figure 5.14 has an amplitude of 50mV. Unfortunately there are some glitches, but the signal is amplified and that is what the amplifier is supposed to do. The averaging is not exactly in the middle of the signal. To see is that an average is made, which is good. Also the average is very flat, what makes the detection of the signal by the comparator even better. But a lower average is recommended to have the correct duty-cycle.

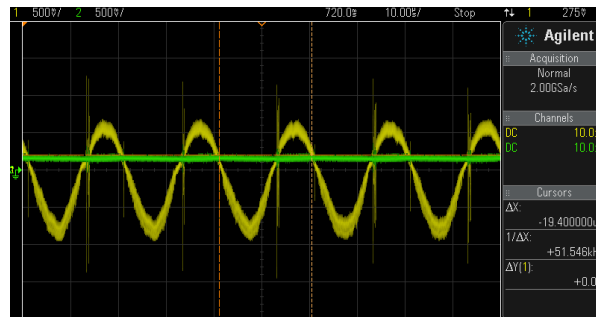


Figure 5.15: Filtered signal before amplifier in the LF-backend

Measurement results Comparator The comparator works also very well. In figure 5.16 we see that the comparator makes a good square wave of the signal. As already mentioned in the paragraph above, the duty-cycle is not 50%. But that is due to the averaging, not to the comparator. The square waves have a good slew-rate, it is very steep and amplified to the maximum voltage of the comparator(which is 1.5V). The glitches in the signal still are annoying. The glitches make it difficult for example, a microcontroller to detect a 0 or 1. Because the ramp of the square wave is not stable.

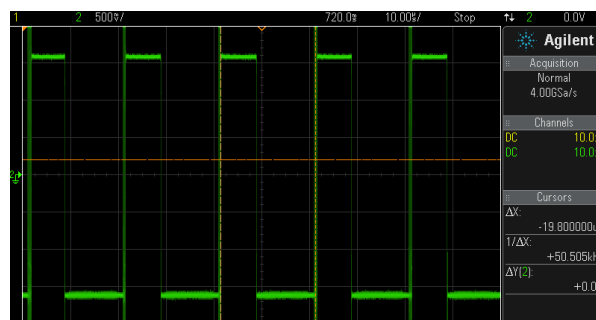


Figure 5.16: Filtered signal before amplifier in the LF-backend

6

CONCLUSIONS AND FUTURE WORK

In this chapter the final results will be compared to the requirements stated in 1.1.1. Conclusions are drawn from this comparison. Of course there are things that can be optimized and this will be discussed in 6.2.

6.1. CONCLUSIONS

In this work the aim of the project was to design a receiver for the AWSN mentioned in 6.2, and to design a applicable coil for the energy harvesting as proposed.

Calculations and simulations for the coil design were done. From these calculations and simulations two designs were presented.

The RF-frontend of the receiver has been tested. The noise figure of the overall RF-frontend is good. The gain is slightly below the requirement but by measurements we verified that it is still enough for our application.

Because of the later detected TV bands that are close to the band of our interest there has to be filtered. A filter has been chosen and after measurement it worked very well.

To detect the signal an dedicated IC is used. Even it could not be simulated, after measurements it worked very well. The whole RF-frontend is measured including the envelope detector. The whole circuitry is working very well. The signal is amplified and the information in the signal is detected.

The LF-backend is working well, besides the buffer, and the averaging. The amplifier and band-pass filtering, including the DC decoupling is working. Also the comparator shows a good result. The buffer needs to be changed because the buffer now used, is not working properly. The buffer is not working in the simulations as at the measurements. The averaging is a little to high, that there will not be a duty cycle of 50%. Even though these things are not working properly the other parts of the LF-backend are working.

6.2. RECOMMENDATIONS

From the conclusions some recommendations were derived for future work.

- **Coil**

The coil is not manufactured. To verify the proposed designs and to verify the calculations it is needed that a coil is made. Than conclusions can be drawn on which formula is the most exact and the AWSN can be tested in a practical environment.

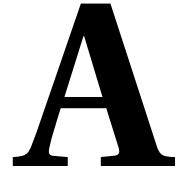
- **Receiver**

The complete test with the AWSN is not done yet. To verify if the receiver is also capable of working with the AWSN this measurement is really needed. Now there is only tested with clean signals but the signal from the AWSN shall be more noisy. It will also have to be considered that there is a lot of noise interfering with our receiver. Because of the noise, the measurements were a little bit affected.

The buffer is not working properly at the moment. There should be made use of an other buffer which doesn't affect the signal. Probably the LF-backend will work better.

To have a duty cycle of 50% the averaging circuit has to be changed a little bit. Probably a change in the cutoff frequency will solve the problem.

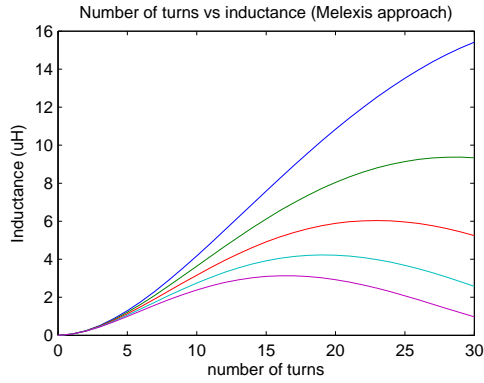
The receiver should be capable, with some adjustments, of receiving the ECG signal from an other AWSN node. To have a more wider useable receiver this potentiality should be investigated.



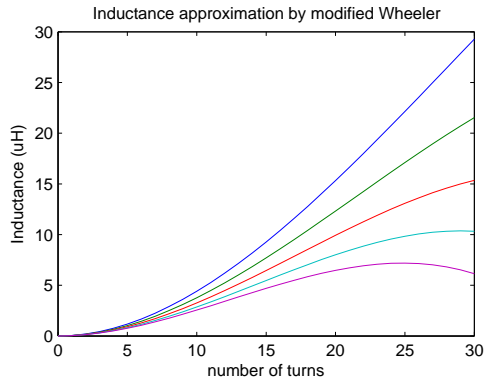
COIL SIMULATION AND CALCULATION RESULTS

For different size and shape of coils some simulations were done to see which design satisfy our requirements. But before the simulations were done, some calculations have been made. In figure the inductance calculation results are shown, and in figure the AC resistance calculation is shown. In table [A.1](#) and table [A.2](#) the simulation results for simulating a hexagonal coil and for a circled coil are stated.

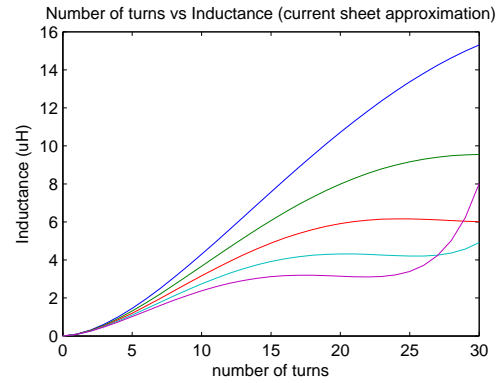
Inductance calculation results:



(a) Use of Melexis formula to calculate circular coils inductance for different turns, trace width and trace spacing

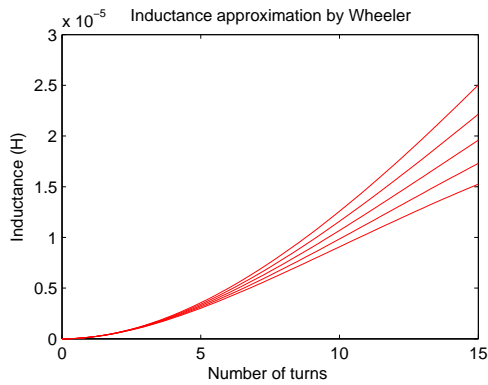


(b) Use of modified Wheeler formula to calculate hexagonal coils inductance for different turns, trace width and trace spacing

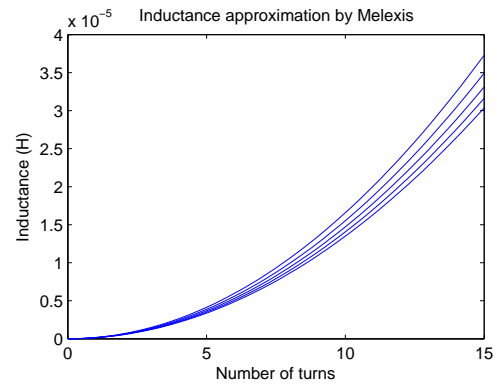


(c) Use of Current Sheet approximation formula to calculate circular coils inductance for different turns, trace width and trace spacing

Figure A.1: Calculated inductance for circular coils with different approaches



(a) Use of Melexis formula to calculate coils inductance for different turns, trace width and trace spacing



(b) Use of Melexis formula to calculate coils inductance for different turns, trace width and trace spacing

Figure A.2: Calculated inductance for rectangular coils with different approaches

Table A.1: Simulation results of energy harvesting coil in circled and hexagonal shape

Shape	N ¹	w ²	s ³	L ⁴	C ⁵	X _C ⁶	R _e ⁷	R ⁸	X _L ⁹	f _{res} ¹⁰	f ¹¹
circle	25	0.15	0.24	10.09	7.22	1.58	7.03	6.26	887.13	5.90	1.40
circle	30	0.15	0.24	10.30	6.83	1.66	8.01	7.16	906.47	6.00	1.40
hex.	25	0.15	0.18	22.49	9.19	1.24	18.56	13.10	1978.51	3.50	1.40
hex.	18	0.15	0.18	8.57	8.79	1.29	6.81	6.04	753.80	5.80	1.40
hex.	20	0.15	0.18	9.62	8.39	1.35	7.55	6.63	846.65	5.60	1.40
hex.	18	0.15	0.17	8.81	8.85	1.28	7.01	6.19	774.72	5.70	1.40
hex.	18	0.15	0.16	9.05	8.92	1.27	7.21	6.34	796.37	5.60	1.40
hex.	18	0.15	0.15	9.31	9.33	1.22	7.45	6.48	818.84	5.40	1.40
hex.	20	0.15	0.15	22.9	9.19	1.24	18.56	13.10	1978.51	3.50	1.40
hex.	19	0.15	0.15	9.94	9.07	1.25	7.90	6.84	874.58	5.30	1.40
hex.	22	0.15	0.19	10.23	7.89	1.44	7.97	7.01	900.04	5.60	1.40
hex.	19	0.15	0.16	9.65	9.00	1.26	7.64	6.65	849.16	5.40	1.40
circle	22	0.15	0.22	9.64	7.81	1.45	7.06	6.26	847.56	5.80	1.40
circle	21	0.15	0.22	9.27	7.85	1.45	6.81	6.06	815.76	5.90	1.40

Table A.2: Simulation results of energyharvesting coil in rectangle shape

Shape	W ¹²	l ¹³	N ¹	w ²	s ³	L ⁴	C ⁵	X _C ⁶	R _e ⁷	R ⁸	X _L ⁹	f _{res} ¹⁰	f ¹¹
rect.	19	72	7	0.15	0.15	6.44	2.13	5.34	7.51	6.00	566.43	4.30	1.40
rect.	19	72	9	0.15	0.15	10.22	2.15	5.30	12.05	8.31	898.59	3.40	1.40
rect.	19	72	8	0.15	0.15	8.22	2.13	5.33	9.57	7.15	723.01	3.80	1.40
rect.	19	72	10	0.15	0.16	12.19	2.03	5.60	14.51	9.49	1072.20	3.20	1.40
rect.	19	72	10	0.15	0.18	11.74	1.98	5.74	13.62	9.16	1032.30	3.30	1.40
rect.	19	72	10	0.15	0.2	11.32	1.94	5.87	12.86	8.87	995.39	3.40	1.40
rect.	19	72	10	0.15	0.24	10.56	1.85	6.14	11.67	8.41	928.61	3.60	1.40
rect.	19	72	8.75	0.15	0.15	9.40	2.08	5.47	10.99	7.91	826.60	3.60	1.40
rect.	19	72	8.5	0.15	0.15	9.23	2.12	5.37	10.77	7.76	811.55	3.60	1.40
rect.	19	72	8.25	0.15	0.15	8.39	2.21	5.16	9.78	7.18	738.11	3.70	1.40
rect.	19	72	8.5	0.15	0.16	9.08	2.15	5.28	10.48	7.55	798.52	3.60	1.40

¹²width rectangle in mm¹³length of the rectangle in mm¹number of turns²trace width in mm³spacing between traces in mm⁴Inductance of the coil in $E - 6H$ ⁵Capacitance of the coil in $E - 12F$ ⁶Capacitive reactance in $\Omega E + 3$ ⁷Resistance⁸Resistance in Ω ⁹Inductive reactance in Ω ¹⁰Resonance frequency used in simulation in $E + 7Hz$ ¹¹frequency of the coil in $E + 7Hz$

BIBLIOGRAPHY

- [1] W. S. Andre Mansano, Sumit Bagga, *A 1.5 13.56 402 mhz autonomous wireless sensor node with temperature monitoring in 0.18 cmos*, accepted for publishing in ESSCIRC (2014).
- [2] K. Ashton, *That 'internet of things' thing, in the real world things matter more than ideas.* (2009).
- [3] Melexis, *Antenna Design for MLX90129*, Melexis, application note ed.
- [4] Y. Lee, *Antenna circuit design for RFID applications*, Microchip, an710 ed.
- [5] S. S. Mohan, M. del Mar Hershenson, S. P. Boyd, and T. H. Lee, *Simple accurate expressions for planar spiral inductances*, Solid-State Circuits, IEEE Journal of **34**, 1419 (1999).
- [6] S. Salleh, K. Salleh, M. F. Hashim, and Z. A. Majid, *Design and analysis of 13.56 mhz rfid antenna based on modified wheeler equation: A practical approach*, in *Electronic Devices, Systems and Applications (ICEDSA), 2010 Intl Conf on* (IEEE, 2010) pp. 326–330.
- [7] C. Turner, *Backscatter modulation of impedance modulated rfid tags*, (2003).